Jean-Marie Beaulieu

[BeaulieuJM.ca/publi/Bea2004a]

Segmentation of Textured Polarimetric SAR Scenes by Likelihood Approximation

Authors: **Beaulieu** Jean-Marie, Ridha Touzi

Journal: IEEE Transactions on Geoscience and Remote Sensing

2004, vol. 42, issue 10, p. 2063–2072

ISBN: 0196-2892

URL: https://ieeexplore.ieee.org/document/1344159

DOI: 10.1109/TGRS.2004.835302

Abstract: A hierarchical stepwise optimization process is developed for polarimetric synthetic aperture radar image segmentation. We show that image segmentation can be viewed as a likelihood approximation problem. The likelihood segment merging criteria are derived using the multivariate complex Gaussian, the Wishart distribution, and the K-distribution. In the presence of spatial texture, the Gaussian-Wishart segmentation is not appropriate. The K-distribution segmentation is more effective in textured forested areas. The validity of the product model is also assessed, and a field-adaptable segmentation strategy combining different criteria is examined.

“Segmentation of Textured Polarimetric SAR Scenes by Likelihood Approximation,”
Beaulieu Jean-Marie, Ridha Touzi,
IEEE Transactions on Geoscience and Remote Sensing, vol. 42, iss. 10, p. 2063–2072, 2004.

DOWNLOAD **from the Publisher**
DOWNLOAD **from from Academia** **(open access)**

INSPEC Accession Number: 8165108
DOI: 10.1109/TGRS.2004.835302
Date of Publication : Oct. 2004
Date of Current Version : 18 octobre 2004
Issue Date : Oct. 2004
Sponsored by : IEEE Geoscience and Remote Sensing Society
Publisher: IEEE

Segmentation of textured polarimetric SAR scenes by likelihood approximation

Jean-Marie Beaulieu, *Member, IEEE*, and Ridha Touzi, *Member, IEEE*

***Abstract*— A hierarchical stepwise optimization process is developed for polarimetric SAR image segmentation. We show that image segmentation can be viewed as a likelihood approximation problem. The likelihood segment merging criteria are derived using the multivariate complex Gaussian, the Wishart distribution, and the K-distribution. In the presence of spatial texture, the Gaussian-Wishart segmentation is not appropriate. The K-distribution segmentation is more effective in textured forested areas. The validity of the product model is also assessed and a field adaptable segmentation strategy combining different criteria is examined.**

***Index Terms*—Hierarchical image segmentation, maximum likelihood estimation, polarimetric SAR image, texture, Wishart and K distributions.**

I. Introduction

In remote sensing, a segmentation process can be used to detect land fields and to improve pixel classification. In classification, a class number is assigned to each pixel. A segmentation process divides the image into distinct and self-similar regions. The segmentation of SAR (Synthetic Aperture Radar) images is greatly complicated by the presence of coherent speckle. The complex structure of the SAR images requires the utilization of complex processes for segmentation and classification. They are based on scene and speckle models. There are well accepted models for 1 channel SAR images [1]. The speckle amplitude of homogeneous areas is represented by the Rayleigh distribution. The K-distribution is used to model the backscattered radar intensity from a Gamma distributed scene such as forested areas [1]. Other distributions, such as the Weibull or the Lognormal distributions, are used to model various textures of SAR images [1].

Kong *et al.* [2] were the first to show that the full polarimetric measurements provide better classification and segmentation than single channel measurements. The probability density function (pdf) of a complex Gaussian vector was used to derive the classification measure that optimizes the likelihood ratio test [2]-[4]. Lee *et al.* [5] use the Wishart distribution to derive a classification measure that can be applied to multi-look data. Skriver *et al.* [6] introduced a likelihood ratio test method for segmentation of polarimetric SAR images.

The methods currently used for classification or segmentation of polarimetric SAR images are based on multivariate complex Gaussian or Wishart models. Such distributions are not appropriate for textured areas. In this study, a new segmentation method uses the K-distribution model to better preserve the Gamma-distributed texture.

The main approaches to image segmentation are based upon classifications, edges or regions. Image segmentation can result from the classification or the labeling of each pixel. The main process is the classification of pixels where the spatial aspect is not usually considered [7]. The image partition is a side effect of the classification. Markov random field and texture models have been used to include the spatial aspect into the class probabilistic models [8], [9]. An edge detection process can also be used to define segment boundaries [10]-[14]. Watershed segmentation algorithms use gradient images [15], [13].

We consider that true image segmentation processes are based upon regions. The goal of the process is to identify regions (segments) that satisfy some criteria. Spatial aspects are involved in the criteria. A typical agglomerative approach involves the sequential merging of regions [6], [16]-[18]. The first techniques used threshold-based decision. More powerful techniques now use iterative optimization processes [19]-[22].

Segmentation consists of the sequential merges of similar segments. Development of a segmentation process involves the definition of an appropriate segment similarity measure. A probabilistic approach is often used. The similarity measure is related to testing if the 2 segments belong to the same population. Likelihood ratio test is often used [6], [16]. For example, for the polarimetric complex Wishart distribution model, the equality of the covariance matrices is tested. Similar measures are used in pixel or region classification. However, in segmentation, the sizes of segments vary which introduces difficulties and differentiates it from classification. In classification, we have reliable class statistics again with

Manuscript received September 30, 2003.

J.-M. Beaulieu is with the Computer Science and Software Engineering Department, Laval University, Quebec City, Quebec, G1K-7P4, Canada (phone: 418-656-2131 ext. 2564; fax: 418-656-2324; e-mail: jean-marie.beaulieu@ift.ulaval.ca). Part of this work was completed while Professor J.M. Beaulieu was in sabbatical year at the Canada Centre for Remote Sensing, Ottawa, Canada.

R. Touzi is with the Canada Centre for Remote Sensing, Natural Resources Canada, 588 Booth St., Ottawa, Ontario, K1A-0Y7, Canada (e-mail: Ridha.Touzi@ccrs.nrcan.gc.ca).

the pixel or region statistics are compared. In segmentation, the statistics of 2 segments are compared and the result could be quite unreliable if the segments are small. Furthermore, the evaluation is a difficult problem in segmentation. The goal is to divide the image into distinct self-similar regions. Classification error can not generally be used. This paper proposes a likelihood approximation approach. A likelihood measure of a partition is defined and used as a global objective function to optimize. In the hierarchical segmentation framework, the local segment merging criterion is derived from the global criterion. This ensures that each merging step does its best to optimize the global criterion.

The next section presents a hierarchical segmentation algorithm based upon stepwise optimization. Image segmentation is then presented as a likelihood approximation problem. The stepwise optimization criterion is derived from the global likelihood partition measure. Segmentation of homogeneous polarimetric SAR images is examined in Section IV. Stepwise criteria are derived for the multidimensional complex Gaussian distribution and the complex Wishart distribution. Segmentation of textured image is examined in Section V. The segmentation criterion is derived for the K distribution. Segmentation results are then presented for Convair-580 polarimetric SAR data using the Wishart and K-distribution criteria. The partition log likelihood value is used for partition evaluation. Its variation with the partition size (number of segments) is shown. The last section discusses the validity of the different models. The segmentation strategy should self-adapt to the image field characteristics.

II. HIERARCHICAL SEGMENTATION

A. Region merging

A segmentation is a partition P of the image plane I into k disjoint regions $S_i \subseteq I$ such that $P = \{ S_1, S_2 \ldots S_k \}$, $S_i \cap S_j = \varnothing$ for $i \neq j$ and $\bigcup$. A region merging approach starts from small segments and sequentially merges them to produce larger segments [23], [24], [6], [16], [17]. The initial segments can contain only one pixel. A logical predicate, $LP()$, is used to decide if two adjacent segments could be merged. S_i and S_j are merged if $LP(S_i \cup S_j)$ is true. For example, two segments are merged if the module of the mean difference is smaller than a threshold value. The algorithm stops when no more segments could be merged. Different partitions are produced by varying the threshold or the logical predicate parameters. The order of the comparisons has an important effect on the result. Different strategies can be used to guide the order of merges.

B. The Hierarchical Stepwise Optimization algorithm

In pattern recognition, the agglomerative hierarchical clustering algorithm is a generally used technique. It is based upon stepwise optimization: at each iteration, the two most similar clusters are selected and merged. The result of the clustering can be represented by a tree that reflects the hierarchical structure of the data. The addition of the hierarchical structure to a uniform (mean value) segment model provides a better description of remote sensing images. Crop fields and forest areas are composed of subparts that could be decomposed again [17].

A segmentation algorithm derived from hierarchical clustering is now presented [25]. A segment similarity measure, $SC_{i,j}$, is defined as the stepwise criterion to optimize. The algorithm can be defined as follows:

i) Define an initial image partition.
ii) For each adjacent segment pair, (S_i, S_j), calculate the stepwise criterion, $SC_{i,j}$; then find and merge the segments with the minimum criterion value.
iii) Stop, if no more merges are needed; otherwise, go to ii).

We call the algorithm "hierarchical segmentation" to stress the fact that the complete tree is calculated and meaningful partitions at any resolution level can be obtained by cutting the tree at the appropriate level. For example, partitions with 500 to 5000 segments could be considered for a 1000x1000 image.

Many different merging strategies and ways of defining the merging order have been proposed [16]-[18], [6], [13]. A segmentation method based on a combination of radiometric and geometric criteria that permits to create a hierarchical network of regions with a predefined number of resolution levels is described in [17]. Different merging orders are examined in [18]. A segment hierarchy can also be produced by watershed segmentation algorithms [15], [13].

C. Global objective function

Image segmentation can be presented as an optimization problem: find the partition P that optimizes a global objective function $GOF(P)$. Segmentation techniques could limit the choice of GOF. It is particularly difficult to establish a relation between the GOF and local decisions (logical predicate or stepwise criterion). For example, the mean squared error around segment means can be used as GOF. In a hierarchical segmentation framework, the corresponding stepwise criterion was derived in [25]. In the next section, we extend this approach to the case where a segment is described by an arbitrary probability density function. The stepwise criterion is derived for a global likelihood estimation or approximation problem.

III. IMAGE SEGMENTATION AS A LIKELIHOOD APPROXIMATION PROBLEM

Image segmentation can be viewed as the transformation of the original image into a more abstract description. The image is represented by a set of regions or segments. Each segment is described by a set of parameters.

A. Maximum likelihood approach

Following a statistical approach, the image segmentation can be presented as a maximum likelihood estimation problem. Let $\boldsymbol{x}_i$ be the value of pixel i. The probability density function (pdf) of $\boldsymbol{x}_i$ is a function of the segment S that contains the pixel i, ($i \in S$). The pdfs are described by a set of parameters, θ. For the segment S, the pdf of $\boldsymbol{x}_i$ is $p(\boldsymbol{x}_i \mid \theta_S)$. We assume that the pdf of $\boldsymbol{x}_i$ is only function of θ_S and is conditionally independent of other pixel values. Let X be the set of pixel values for the whole image, $X = \{ \boldsymbol{x}_i \mid i \in I \}$. Let Θ_P be the set of all θ_S for the partition P, $\Theta_P = \{ \theta_S \mid S \in P \}$. The likelihood function of Θ_P and P given X is

$$L(\Theta_P, P \mid X) = p(X \mid \Theta_P, P) . \tag{1}$$

We could write the equation as a product of pixel pdfs and take its logarithm.

$$\ln\left(L(\Theta_P, P \mid X)\right) = \sum_{i \in I} \ln\left(p(x_i \mid \theta_{S(i)})\right)\Big|_P \tag{2}$$

$S(i)$ is the segment containing the pixel i and the parameters are evaluated for the partition P. In the maximum likelihood approach, we want to find the partition P and the segment descriptive parameters Θ_P that optimize the likelihood function.

B. Best parameter evaluation

For a segment S, the parameters θ_S can usually be evaluated from statistics calculated over the segment. For a given partition P, the log likelihood function value for the best parameters Θ_P could be defined as $LLF(P)$ and could be calculated rapidly. The function could be written as a sum of the maximum log likelihood values (MLL) for each segment:

$$\begin{aligned} LLF(P) &= \sum_{i \in I} \ln\left(p(x_i \mid \theta_{S(i)})\right) \\ &= \sum_{S \in P} \sum_{i \in S} \ln\left(p(x_i \mid \theta_S)\right) \\ &= \sum_{S \in P} MLL(S) \end{aligned} \tag{3}$$

where

$$MLL(S) = \sum_{i \in S} \ln\left(p(x_i \mid \theta_S)\right) . \tag{4}$$

Equation (3) shows that the difficult part of the optimization process is to find the best partition. Once we have a partition, it is easy to calculate the best descriptive parameters for this partition.

C. Finding the best partition

The importance of the number of segments k in the maximization of $LLF(P)$ must be stressed. Let P_k be the best partition with k segments. Then, the $LLF(P_k)$ function is monotonically nondecreasing with increasing number of segments for P_k (Fig. 1). The number of possible partitions is usually very large for any k value. It would therefore be prohibitive or impossible to find the true global optimum partition P_k. There are two limit cases. When there is one pixel per segment, the number of segments is equal to n, the number of pixels in the image. There is only one possible partition with n segments. This partition has the highest log likelihood value. The log likelihood value can only decrease or stay unchanged when we decrease the number of segments. The other limit case is when k equal one. There is only one partition with one segment (the whole image) and this partition has the lowest log likelihood value.

In hierarchical segmentation, we start with an initial partition P_n and then produce a sequence of partitions $P_n \ldots P_{k+1}, P_k \ldots P_1$ by merging two adjacent segments at each iteration. The partition P_k is produced by merging two segments of P_{k+1}. Let D_q be the decrease of the log likelihood value from P_{q+1} to P_q.

$$D_q = LLF(P_{q+1}) - LLF(P_q) \tag{5}$$

The value of $LLF(P_k)$ could be related to the values of D_q for $q = k \ldots n\text{-}1$.

$$LLF(P_k) = LLF(P_n) - \sum_{q=k}^{n-1} D_q \tag{6}$$

To maximize $LLF(P_k)$, we need to minimize each term D_q of the summation (Fig. 2). This is the goal of the stepwise optimization process. The stepwise criterion can be derived from the minimization of D_q. The P_k partition produced by the stepwise optimization algorithm is not a global optimum. We have not explored all the partitions with k segments. The stepwise optimization only examines the partitions produced by merging two adjacent segments of the P_{k+1} partition. The number of examined cases is equal to the number of adjacent segment pairs in the P_{k+1} partition. The stepwise optimization algorithm is a sub-optimum approach with the hierarchical segment merging constraint.

D. Stepwise criterion

At each iteration, the stepwise optimization algorithm should merge the two segments that produce the smallest decrease of the log likelihood function. For the partition P_{k+1}, $LLF(P_{k+1})$ is equal to the sum of $MLL(S)$ for all segments of P_{k+1} (see (4)). If we consider the merging of segment S_i and S_j from partition P_{k+1} to produce the segment S_u ($= S_i \cup S_j$) in partition P_k then the difference between $LLF(P_{k+1})$ and $LLF(P_k)$ will only involve the segments S_i, S_j and S_u.

$$SC_{i,j} = MLL(S_i) + MLL(S_j) - MLL(S_u) \tag{7}$$

$SC_{i,j}$ is the stepwise criterion. At each iteration, we should

merge the segments that minimize this criterion.

IV. SEGMENTATION OF POLARIMETRIC SAR IMAGE

A. One-look and multi-look speckle models for a homogeneous (non textured) scene

One-look polarimetric SAR images are generally provided under the scattering matrix format. For a reciprocal medium, the cross-polarization hv and vh are identical and the backscattered radar signal from each resolution cell might be characterized by the tri-dimensional vector $\boldsymbol{x}$, $\boldsymbol{x} = (hh,\ hv,\ vv)^T$, where *hv* denote a transmitting antenna horizontally polarized and a receiving antenna vertically polarized. For a fully developed speckle in a homogeneous (spatial texture free) area, $\boldsymbol{x}$ might be assumed to be a zero mean circular complex Gaussian process with a probability density function (pdf) given by [26]:

$$p(x\,|\,\Sigma) = \frac{1}{\pi^3 |\Sigma|} \exp\left(-x^H \Sigma^{-1} x\right) \tag{8}$$

where $\Sigma = E[\,\boldsymbol{x}\,\boldsymbol{x}^H]$ is the covariance matrix, $E[\ ]$ denotes the expectation operator and the superscript H indicates the complex conjugate transpose. This model was first used by Kong *et al.* [2] as the basis for their polarimetric classification process developed for 1-look SAR images.

Polarimetric SAR data might also be provided under the multi-look format. Each single look scattering matrix is transformed into a Mueller matrix, and the average of the L single-look Mueller matrices is assigned to each multi-look pixel [27]. The L-look averaged Mueller matrix is completely characterized by L-look covariance matrix $Z = <\boldsymbol{x}\,\boldsymbol{x}^H>$, and each pixel k should be represented by its L-look covariance matrix, Z_k. The pdf of Z_k was derived in [26] under the assumption that speckle is fully developed and is a zero mean circular complex Gaussian process. The Z_k pdf is the Wishart distribution [26],

$$p(Z_k\,|\,\Sigma) = \frac{|Z_k|^{L-3} \exp\left\{-L\,tr\left(\Sigma^{-1} Z_k\right)\right\}}{Q(L)\,|\Sigma|^L} \tag{9}$$

with

$$Q(L) = \pi^3\,\Gamma(L)\Gamma(L-1)\Gamma(L-2)/L^{3L} \tag{10}$$

The Wishart distribution has been widely used as the basis of classification and segmentation methods for multi-look SAR data [6], [8].

B. One-look polarimetric stepwise criterion

For the segmentation of one-look polarimetric images, we use (8) and consider that the vectors $\boldsymbol{x}$ are the pixel values and the segment descriptive parameters are the covariance matrices. For a segment S with n_S pixels, the best estimate of the parameter Σ is the sample covariance matrix, C.

$$C_S = \hat{\Sigma} = \frac{1}{n_S} \sum_{x \in S} x\,x^H \tag{11}$$

Knowing the best estimate value for a region S, we combine (4), (8) and (11) to obtain the maximum likelihood value for this segment.

$$\begin{aligned} MLL(S) &= \sum_{x \in S} \ln\left(\frac{1}{\pi^3 |C_S|} \exp\left(-x^H C_S^{-1} x\right)\right) \\ &= \sum_{x \in S} \left[-\ln|C_S| - \ln \pi^3 - x^H C_S^{-1} x\right] \\ &= -n_S \ln|C_S| - n_S \ln \pi^3 - \sum_{x \in S} x^H C_S^{-1} x \\ &= -n_S \ln|C_S| - n_S \ln \pi^3 - 3n_S \end{aligned} \tag{12}$$

We obtain the stepwise criterion for merging segments S_i and S_j by substituting (12) into (7).

$$SC_{i,j} = (n_i + n_j) \ln|C_{Si \cup Sj}| - n_i \ln|C_{Si}| - n_j \ln|C_{Sj}| \tag{13}$$

n_i and n_j are the sizes of segments S_i and S_j. At each iteration, the hierarchical segmentation algorithm merges the two segments that minimize this criterion.

C. Segmentation of multilook polarimetric image

In hierarchical segmentation, the merging process starts from an initial partition. For one-look images, it is difficult to start from one-pixel segments. The image can be divided into disjoint cells of L pixels and these cells will define the initial partition. These cells can be viewed as the pixels of a L-look image. Therefore, for L-look image, we can use the stepwise criterion of (13) where n_i is the number of pixels of segment S_i multiplied by the number of looks. n_i represents the number of signal samples inside segment S_i.

We can also derive the stepwise criterion from the Wishart distribution of covariance matrices (9). The best likelihood estimate of Σ for the segment S is

$$C_S = \frac{1}{m_S} \sum_{k \in S} Z_k \tag{14}$$

where m_S is the number of pixels in segment S. The maximum log likelihood value of segment S is

$$\begin{aligned} MLL(S) &= \sum_{k \in S} \ln\left(p(Z_k\,|\,C_S)\right) \\ &= -Lm_S \ln|C_S| + (L-3) \sum_{k \in S} \ln|Z_k| \\ &\quad - 3Lm_S - m_S \ln\left(Q(L)\right) \end{aligned} \tag{15}$$

The stepwise criterion is

$$\begin{aligned} SC_{i,j} &= MLL(S_i) + MLL(S_j) - MLL(S_i \cup S_j) \\ &= L(m_i + m_j) \ln|C_{Si \cup Sj}| - Lm_i \ln|C_{Si}| - Lm_j \ln|C_{Sj}|. \end{aligned} \tag{16}$$

This criterion is equivalent to (13) where $n_i = L\, m_i$.

D. Comparison with hypothesis testing

A statistical hypothesis testing approach can be employed for image segmentation. The likelihood ratio test has been used by many authors for SAR image segmentation [6], [16]. The segmentation method proposed in this paper is equivalent to region merging based on likelihood ratio test with an optimized merging order, where the least different couple of neighboring regions (according to the test) is merged in each step [6], [16]. For polarimetric images, two segments can be merged if their covariance matrices are not significantly different, which means that the observed sample covariance matrices are likely to belong to the same population. The test statistic is then equivalent to $SC_{i,j}$ of (16), [6], [28].

V. Textured Scene and K Distribution

The complex Gaussian and Wishart distributions were derived to model pure fully developed speckle that is a zero mean complex circular Gaussian process. At the presence of spatial texture, the circular Gaussian assumption is no longer valid, and both the complex Gaussian and Wishart models cannot be used. In textured areas, the "polarimetric" product model, which was first introduced by Yueh *et al.*, is currently the most used speckle-scene model [29], [30].

A. K-distributed covariance matrix

For textured areas, the product model was used in [31], [32], [1] to derive the statistics of the covariance matrix Y_k for a gamma-distributed scene signal:

$$p(Y_k \mid \alpha, \Sigma) = \frac{(\alpha L)^{\frac{3L+\alpha}{2}} |Y_k|^{L-3}}{R(L)\,\Gamma(\alpha)\,|\Sigma|^{L}\, tr\left(\Sigma^{-1}Y_k\right)^{\frac{3L-\alpha}{2}}} \times K_{3L-\alpha}\left\{2\sqrt{\alpha L\, tr\left(\Sigma^{-1}Y_k\right)}\right\} \tag{17}$$

with

$$R(L) = \tfrac{1}{2}\,\pi^3\,\Gamma(L)\Gamma(L-1)\Gamma(L-2), \tag{18}$$

where α is the texture shape parameter and Σ is the covariance of the speckle without texture. K_ν is the modified Bessel function.

B. Stepwise Criterion

The segmentation stepwise criterion for the product model could be derived from (4), (7) and (17). After removing the terms that will be cancelled in the stepwise criterion, the maximum log likelihood value for segment S is

$$\begin{aligned} MLL(S) \simeq & \quad + \hat{\alpha})\,\ln(\hat{\alpha}L) \\ & - n\ln(\Gamma(\hat{\alpha})) - nL\ln(|C|) \\ & - \tfrac{1}{2}(3L-\hat{\alpha})\sum_{Y_k \in S}\ln\left\{tr\left(C^{-1}Y_k\right)\right\} \\ & + \sum_{Y_k \in S}\ln\left\{K_{3L-\hat{\alpha}}\left(2\sqrt{\hat{\alpha}L\, tr\left(C^{-1}Y_k\right)}\right)\right\} \end{aligned} \tag{19}$$

n is the size of segment S. $\hat{\alpha}$ and C are the best likelihood estimates of α and Σ for the segment S, i.e. the values that maximize (19). Unfortunately, there is no closed form analytical solution for the parameter estimates [33]. A numerical solution can be computed, but the computing time will be excessive for the segmentation process. We should stress that (19) involve summations over all pixels Y_k of the segment S. The computing time grows with the size of the segment. This was not the case for (16) with the Wishart distribution.

Alternate approximate solutions have been proposed [34]. The population speckle covariance matrix could be approximated by the sample covariance matrix, i.e. by the segment mean value of the signal covariance matrices.

$$C = \frac{1}{n_S}\sum_{k \in S} Y_k \tag{20}$$

The shape parameter α is estimated by the method of moment (MoM) [34]. From the 1-look data, we calculate the variation coefficients CV from the intensity of the *hh*, *hv* and *vv* components over the segment. The shape parameter α is estimated by

$$\hat{\alpha} = 2/(CV^2 - 1) \tag{21}$$

VI. High Resolution Segmentation

The processing of polarimetric SAR images is difficult because of the large variance of the speckle multiplicative noise. We need to average over a large set of homogeneous pixels in order to obtain accurate measures. In hierarchical image segmentation, the resolution of the final partition is defined by the size of the initial segments. To have a good resolution, the initial segments should have few pixels. The sample covariance matrices of those segments will be very noisy. It will be difficult then to discriminate between regions with small value differences. To improve the results, we combine segment shape measures with the stepwise criterion. The covariance matrix model should also be adapted to small segments.

A. Covariance matrix model

The covariance matrix is defined by 3 real values (diagonal elements) and 3 complex values (correlation elements). The determinants of the sample covariance matrices are used in the stepwise criterion $SC_{i,j}$ of (16). When segments contain

only few samples or pixels, the correlation elements of the covariance matrix could be very noisy because of the presence of speckle [38]. Then, the value of the determinant will be unreliable. It is better to use a simpler data model that assumes homogeneous regions with no correlation between the $\boldsymbol{x}$ vector components, $\boldsymbol{x} = (hh, hv, vv)^T$. The criterion is calculated on each channel independently and summed together. This is equivalent to evaluating the determinant with only the diagonal elements. The segmentation process starts with the modified criterion and changes to the full matrix criterion for segment of 20 looks or larger. Weighting factors are used for a gradual transition.

B. Segment shape constraints

In hierarchical segmentation, the accuracy of the decision process is related to the segment sizes. The first merging steps are critical and are error prone because of the small segment sizes and the high noise level of polarimetric and SAR images. If the first segments are not correctly delimited then the following steps will merge segments from different fields and produce contours delimiting speckle artefacts instead of the true field boundaries. Spatial constraints and contour shapes have been used in image segmentation [17], [16]. The effect of the segment merging order on the spatial distribution and size of segments is examined in [18]. Watershed segmentation produces good segment shapes [15], [13]. We use contour shape constraints to improve the first segmentation steps. Details of the measure definitions and operations are given in [22]. We use the segment perimeter, the segment area and the contour length to define 3 contour factors, *Cp*, *Ca* and *Cl*. We define a bounding box containing $S_i \cup S_j$: a rectangle with left and right sides corresponding to the minimum and maximum values of the x coordinate of the segment and with the top and bottom sides corresponding to the minimum and maximum values of the y coordinate. Cp is the perimeter of $S_i \cup S_j$ over the perimeter of the bonding box. Ca is the area of the bonding box over the area of the segment. Let l_{min} be the smallest of the contour lengths of S_i and S_j and l_{com} the length of the common boundary. *Cl* is equal to $(l_{min} - l_{com})/ l_{com}$. For all the examples of Section VII, the stepwise criterion is scaled by the product of the 3 shape factors. Without these factors, the shapes and boundaries of produced segments are not well defined. The segments are not compact. They have irregular shapes with many branches.

VII. RESULTS AND EVALUATIONS

The likelihood approximation approach for image segmentation have been implemented and tested using polarimetric Convair-580 SAR data collected over the Ottawa region, Canada. A test region in the Mer Bleu area is selected. The initial 1-look image has a resolution of 5.6m x 0.63m [39]. The covariance matrices of 9 pixels are averaged in azimuth to form a square pixel image that is presented in Fig. 3 using the amplitude of the hh, vv and hv channels. The image contains crop field areas and forest areas.

A. Homogeneous model

The homogeneous region model is first examined. The segmentation stepwise criterion (16) derived from the Wishart distribution is used. Fig. 4 shows a partition with 2000 segments. It shows that the partition is data driven. We should stress the hierarchical nature of the results and the difficulty to find an appropriate stopping point. For some parts of the image, more merging should have been done while, for other parts, less merging would be needed. Generally, field boundaries are correctly delimited. The segmentation is a difficult task because of the presence of speckle in SAR images. The homogeneous scene criterion seems to give good results for crop fields. More merging is recommended for forest areas.

B. Segmentation evaluation

The likelihood approximation approach looks for the partition that optimizes the likelihood value (2). Therefore, the likelihood value can be used as an evaluation measure [35]. Fig. 5 shows the log likelihood value as a function of the number of segments of the partition. The total log likelihood value is divided by the image size to produce the average per pixel value. The value decreases when the number of segments is decreased by merging. It starts with 480,000 segments of 1 pixel. After 240,000 merges, we have a partition with 240,000 segments with an average size of 2 pixels. The first merges can be done with small decreases of the log likelihood value. The interesting part is for partitions with 500 to 10,000 segments where decreases are more important. Fig. 6 shows that the log likelihood value drops rapidly as segments get bigger. A log scale for the number of segments can provide a better representation, as shown in Fig. 7. The average log likelihood value for the 2000 segment partition is 23.8. The regular shape of the curves suggests that the segmentation process is appropriate to maximize the likelihood value. Similar curves are obtained with the K distribution criterion.

The process gives to the user the choice of the stopping point. The stepwise criterion reflects low level signal description: the speckle statistics. On the other hand, the stopping point is more related to the user objective: what levels of details are needed by the application. The curves show that the user could use the average log likelihood value or the partition size to specify the stopping point.

For a given partition, the log likelihood value can be calculated for each pixel of the image. A normalisation is needed if we want to use the resulting image to visually evaluate the partition. The likelihood corresponds to a probability density that is function of the distribution width. Large likelihood values will be observed in areas where the determinant of the covariance matrix is small. To remove this effect, we “normalize” the pixel values such that the

determinant of the segment covariance matrix is equal to one. For the Wishart distribution, we obtain the normalized log likelihood value of pixel Z_k from (9):

$$LL^*(Z_k) = (L-3)\left(\ln|Z_k| - \ln|C_S|\right) - L\,tr\left(C_S^{-1}Z_k\right) - \ln\left(Q(L)\right) \quad (22)$$

Fig. 8 shows the normalized log likelihood image corresponding to the partition of Fig. 4. There are fluctuations produced by speckle. Information lost produced by assigning pixels to segments with different covariance matrices is also shown as dark linear features or spots. The quality of the segmentation is shown by the limited scope of the information lost.

C. Textured model

For a large part of the image, the homogeneous model is not appropriate. For example, forest areas are usually considered as textured regions. The segmentation stepwise criterion derived from the K distribution has been applied to the polarimetric SAR image. In the forest areas, there are more merging than with the Wishart criterion for partitions with the same number of segments. There are less segments and they are larger. The texture model is able to explain more important fluctuation of backscattered signal and the presence of structure, like the darker zones in the forest areas that could be shadow effects. This flexibility of the model could make it more difficult to discriminate the roads from the surrounding forest.

In order to obtain more valuable results, we should use both criteria: apply the Wishart criterion in homogeneous areas and the K distribution criterion in textured areas. How to combine the two criteria in a hierarchical segmentation process is an open question. We now present a first attempt to show that good segmentation results can be obtained. Further researches are needed to define a well sound process. The texture parameter α is used to discriminate between homogeneous and textured segments. We use a threshold value of 15 with a gradual transition zone of ±5. The Wishart criterion is used if $\alpha > 20$. The K distribution criterion is used if $\alpha < 10$. A weighted combination is used in the transition zone. The result for 2000 segments is shown in Fig. 9. In the forest areas, in the middle of the image, the result is better than in the Wishart partition of Fig. 4. The forest segments are larger. More fragmentation is observed in other areas in order to maintain the same total number of segments. This example shows the advantage of using the K distribution criterion for textured fields.

In both images, there are problems with road detection. Since segmentation is based on statistics computed within areas of stationary scene signals, areas of nonstationary signals, such as curvilinear features, should be treated separately [11]. This was done, for example, by Walessa and Datcu who used a combination of edge detection and region growing in their segmentation [36]. Segmentation with the K distribution criterion required much more computing time than the Wishart criterion, 44.4 minutes versus 10.5 seconds with a Pentium 4 processor, 3.0 gigahertz.

VIII. LIMITATION OF THE K-DISTRIBUTION MODEL

The likelihood segment merging criteria was derived using the K-distribution. This would suppose that:

1. the product model is valid, and
2. the scene signal is Gamma distributed.

The product model assumes that texture is independent of the channel of polarization. Most of the authors have assumed that this is valid [1], [31]. Sheen and Johnson [37] showed experimentally, using polarimetric SAR data, that this statement might not be true. The product model assumption has been assessed here within a forested area using the Convair-580 SAR data set. The coefficient of variation is computed for each channel within sufficiently large windows (more than 1000 independent samples). The dynamic range of the coefficient of variation reaches for given samples 5% to 6%, as seen in Fig. 10. This demonstrates that the texture might be polarization dependent, and as such, the product model assumption is not all the time valid.

Consequently, the product model should be assessed prior to the application of the segmentation. In addition, the scene signal intensity should be Gamma distributed. This property has been accepted for forested areas, and the K-distribution segmentation should be limited to such areas under the condition that the product model is valid. We are developing a segmentation strategy that will self-adapt to the area characteristics. In the future, the likelihood segment merging criteria will be derived for other distributions (lognormal, Weibull …) in order to extend the use of the segmentation algorithm to more varieties of texture, under the product model assumption. The process of combining the different texture models in the segmentation strategy will be carefully examined.

IX. CONCLUSION

A general powerful segmentation approach based upon likelihood approximation has been presented. Its adaptation for segmentation of homogeneous and textured scenes was shown. Better results are obtained with the K-distribution segmentation than with the Gaussian and Wishart distribution within textured areas. The likelihood criteria should be derived for other texture models to extend the application of the segmentation. The product model is only limited to texture that are independent of polarization. A more general model that takes into account polarization texture dependence is currently being developed, and will be integrated in the segmentation to extend its application to a wider range of targets. The most well known classification techniques, which are also based on the Gaussian and

Wishart model, should be also improved by integrating more suitable texture models.

REFERENCES

[1] C. Oliver and S. Quegan, *Understanding Synthetic Aperture Radar Images*, Artech House, Boston, 1998.

[2] J.A. Kong, A..S. Swartz, H. A. Yueh, L.M. Novak, and R.T. Shin, "Identification of terrain cover using the optimum polarimeter classifer," *J. Electromagnetic Waves and Applications*, vol. 2, no. 2, pp. 171-194, 1988.

[3] H.H. Lim, A.A. Swartz, J.A. Kong, R.T. Shin, and J.J. Van Zyl, "Classification of earth terrain using polarimetric synthetic aperture radar images", *J. Geophys. Res.*, vol. 94, pp. 7049-7057, June 1989.

[4] E. Rignot, "Unsupervised segmentation of polarimetric SAR data using the covariance matrix", *IEEE Trans. on Geosci. Remote Sensing*, vol. 30, no. 4, July 1992.

[5] J.S. Lee, M.R. Grunes and R. Kwok, "Classification of multi-look polarimetric SAR imaging based on complex Wishart distributions," *Int. J. Remote Sensing*, vol. 15, no. 11, pp. 2299-2311, 1994.

[6] H. Skriver, J.Schou, A.A.Nielsen and K.Conradsen, "Polarimetric segmentation using the complex Wishart test statistic," in *Proc. IGARSS'02*, Toronto, Canada, 2002.

[7] D.M. Smith, "Speckle reduction and segmentation of Synthetic Aperture Radar images," *Int. J. Remote Sensing*, vol. 17, no. 11, pp. 2043-2057, 1996.

[8] J.S. Lee, M.R. Grunes, T.L. Ainsworth, L.J. Du, D.L. Schuler and S.R. Cloude, "Unsupervised classification using polarimetric decomposition and the complex Wishart classifier," *IEEE Trans. on Geosci. Remote Sensing*, vol. 37, no. 5, pp. 2249-2258, Sept. 1999.

[9] G. Liu, H. Xiong and S. Huang, "Study on segmentation and interpretation of multi-look polarimetric SAR images," *Int. J. Remote Sensing*, vol. 21, no. 8, pp. 1675-1691, 2000.

[10] R. Touzi, A. Lopes and P. Bousquet, "A statistical and geometrical edge detector for SAR image," *IEEE Trans. on Geosci. Remote Sensing*, vol. 26, no. 6, pp. 764-773, Nov. 1988.

[11] R. Touzi, "A review of speckle filtering in the context of estimation theory," *IEEE Trans. on Geosci. Remote Sensing*, vol. 40, no. 11, pp. 2392-2404, Nov. 2002.

[12] J. Le Moigne and J.C. Tilton, "Refining image segmentation by integration of edge and region data," *IEEE Trans. on Geosci. Remote Sensing*, vol. 33, pp. 605-615, 1995.

[13] R. Fjortoft, A. Lopes, P. Marthon and E. Cubero-Castan, "An optimal multiedge detector for SAR image segmentation," *IEEE Trans. Geosci. Remote Sensing*, vol. 36, pp. 793-802, 1998.

[14] R. Caves, S. Quegan and R. White, "Quantitative comparison of the performance of SAR segmentation algorithms," *IEEE Trans. on Image Processing*, vol. 7, no. 11, pp. 1534-1546, Nov. 1998

[15] L. Najman and M. Schmitt, "Geodesic Saliency of Watershed Contours and Hierarchical Segmentation," *IEEE Trans. Pattern Analysis and Machine Intelligence*, vol. 18, no. 12, pp. 1163-1173, 1996.

[16] R. Cook, I. McConnell, C. Oliver and E. Welbourne, "MUM (Merge Using Moments) segmentation for SAR images," in *Proc. SPIE*, vol. 2316, pp. 92-103, 1994.

[17] U.C. Benz, P. Hofmann, G. Willhauck, I. Lingenfelder and M. Heynen, "Multi-resolution, object-oriented fuzzy analysis of remote sensing data for GIS-ready information," *ISPRS Journal of Photogrammetry & Remote Sensing*, vol. 58, pp. 239–258, 2004.

[18] M. Baatz and A. Schäpe, "Multiresolution Segmentation: an optimization approach for high quality multi-scale image segmentation", in *Angewandte Geographische Informationsverarbeitung XII. Beiträge zum AGIT-Symposium Salzburg 2000*, Karlsruhe, Herbert Wichmann Verlag, pp. 12-23, 2000 (http://www.agit.at/papers/2000/baatz_FP_12.pdf).

[19] Y. Dong, B.C. Forester and A.K. Milne, "Segmentation of radar imagery using the Gaussian Markov random field model," *Int. J. Remote Sensing*, vol. 20, no. 8, pp. 1617-1639, 1999.

[20] J. Lira and L. Frulla, "An automated region growing algorithm for segmentation of texture regions in SAR images," *Int. J. Remote Sensing*, vol. 19, no. 18, pp. 3593-3606, 1998.

[21] R. Cook, I. McConnell, D. Stewart, and C. J. Oliver, "Segmentation and simulated annealing," in *Proc. SPIE EurOpto SAR Image Analysis and Modelling II*, Taormina, Italy, vol. 2958, pp. 30-37, 1996.

[22] J.M. Beaulieu, "Utilisation of contour criteria in micro-segmentation of SAR images," *Int. J. Remote Sensing*, to be published.

[23] R.M. Haralick and L. G. Shapiro, "Survey: Image segmentation techniques," *Comput. Vision Graphics Image Process.*, vol. 29, pp. 100-132, 1985.

[24] S.W. Zucker, "Region growing: Childhood and adolescence," *Camput. Graphics lmage Process.*, vol. 5, pp. 382-399, 1976.

[25] J.M. Beaulieu and M. Goldberg, "Hierarchy in picture segmentation: a step-wise optimization approach," *IEEE Trans. on Pattern Analysis and Machine Intelligence*, vol. 11, pp. 150-163, 1989.

[26] J.W. Goodman, "Statistical analysis based on a certain multivariate complex Gaussian distribution," *Ann. Math. Stat.*, vol. 34, no. 152, pp. 152-180, 1963.

[27] P.C. Dubois and L. Norikane, "Data volume reduction for imaging radar polarimetry", in *Proc. IGARR'87*, pp. 691-697, 1987.

[28] K. Conradsen, A.A. Nielsen, J. Schou and H. Skriver, "A test statistic in the complex Wishart distribution and its application to change detection in polarimetric SAR data," *IEEE Trans. on Geosci. Remote Sensing*, vol. 41, no. 1, pp. 4-19, Jan. 2003.

[29] I.R. Joughin, D.B. Percival, and D.P. Winebrenner, "Probability density functions for multilook polarimetric signatures," *IEEE Trans. on Geosci. Remote Sensing*, vol. 32, pp. 562-474, May 1994.

[30] S.H. Yueh, J.A. Kong, J.K. Jao, R.T. Shin, L.M. Novak, and R.T. Shin, "K distribution and terrain radar clutter," *J. Electro. Waves and Appl.*, vol. 3, no. 8, pp. 747-768, 1989.

[31] J.S. Lee, D.L. Schuler, R. H. Lang, and K.J. Ranson, "K-distribution for multi-look processed polarimetric SAR Imagery", in *Proc. IGARSS'94*, Pasadena, CA, pp. 2179-2181, 1994.

[32] A. Lopes and F. Sery, "Optimal speckle reduction for the product model in multilook polarimetric SAR imagery and the Wishart distribution," *IEEE Trans. on Geosci. Remote Sensing*, vol. 35, no. 3, pp. 632-647, May 1997.

[33] I. R. Joughin, D. P. Winebrenner, and D. B. Percival, "Maximum likelihood estimation of K -distributed parameters for SAR data," *IEEE Trans. on Geosci. Remote Sensing*, vol. 31, pp. 989-999, Sept. 1993.

[34] D. Blacknell, "Comparison of parameter estimators for K-distribution," *IEE Proc.-Radar, Sonar Navig.*, vol. 141, no. 1, pp. 45-52, Feb. 1994.

[35] H. Skriver, A.A. Nielsen and K. Conradsen, "Evaluation of the Wishart test statistics for polarimetric SAR data," in *Proc. IGARSS'03*, Toulouse, France, July 2003.

[36] M. Walessa and M. Datcu, "Model-based despeckling and information extrcation from SAR images", *IEEE Trans. on Geosci. Remote Sensing*, vol. 38, pp. 2258-2269, Sept. 2000.

[37] D.R. Sheen and L.P. Johnson, "Statistical and spatial properties of forest clutter measured with polarimetric synthetic aperture radar, *IEEE Trans. on Geosci. Remote Sensing*, vol. 30, pp. 578-588, May 1992.

[38] R. Touzi, A. Lopes, J. Bruniquel and P.W. Vachon, "Coherence Estimation for SAR Imagery;" *IEEE Trans. on Geosci. Remote Sensing*, vol. 37, no. 1, pp. ,135-149, Jan. 1999.

[39] C.E. Livingstone, A.L. Gray, R.K. Hawkins, P.W. Vachon, T.I. Lukowski, and M. LaLonde, "The CCRS airborne SAR systems: Radar for remote sensing research," *Can. J. Remote Sensing*, vol. 21, no. 4, pp. 468–491, 1995.

Jean-Marie Beaulieu (S'83-M'84) received the Bachelor's and Master's degrees in electrical engineering from Sherbrooke University, Sherbrooke, Quebec, Canada, in 1974 and 1976, respectively, and the Ph.D. degree in electrical engineering from Ottawa University, Ottawa, Ontario, Canada, in 1985. From 1985 to 1987, he was working at the National Research Council of Canada for the Public Safety Project Office. He is currently professor in the Department of Computer Science and Software Engineering at Laval University, Quebec, Quebec, Canada. He was visiting professor at the Canada Centre for Remote Sensing, Ottawa, Canada in 1995, 2001 and 2003. His areas of research interest include image processing and analysis, pattern recognition, segmentation of remote sensing images (optical and SAR) and filtering of SAR images.

Ridha Touzi (M'93) received the Ingenieur degree from l'Ecole Nationale de l'Aviation Civile, Toulouse, France, in 1983, and the M.S. degree (DEA and Master) from l'Ecole Nationale Supérieure de l'Aéronautique et de l'Espace, Toulouse, 1984. He received the Ph.D. degree and *le diplôme de l'Habilitation à diriger des recherches* from l'Université Paul Sabatier, Toulouse, France, in 1988 and 1996, respectively. From 1988 to 1990, he was Research Scientist at the Centre d'Etude Spatiale des Rayonnements. From 1990 to 1992, he was with the Canada Centre for Remote Sensing (CCRS) in Ottawa as a Canadian Government Laboratory Visiting Fellow. He was professor at the Royal Military College of St-Jean, Québec, Canada, from 1992 to 1994. In 1994, he jointed CCRS as a research scientist. His research interests include many aspects of SAR image processing, polarimetry, and interferometry. Dr. Ridha Touzi is the recipient of the *1999 Geoscience and Remote Sensing Transactions Prize Paper Award* for the study on the "Coherence Estimation for SAR imagery".

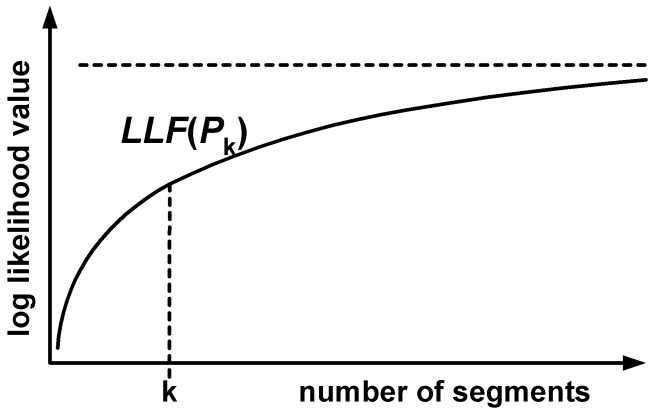

Fig. 1. Log likelihood value of the best partition as a function of the number of segments. The log likelihood value can only decrease or stay unchanged when we decrease the number of segments.

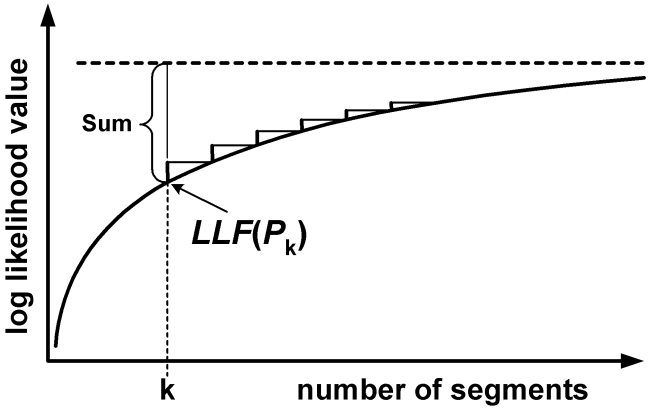

Fig. 2. Maximization of the log likelihood value in hierarchical segmentation. We minimize the decrease of the log likelihood function at each segment merging in order to maximize the log likelihood value of the final partition.

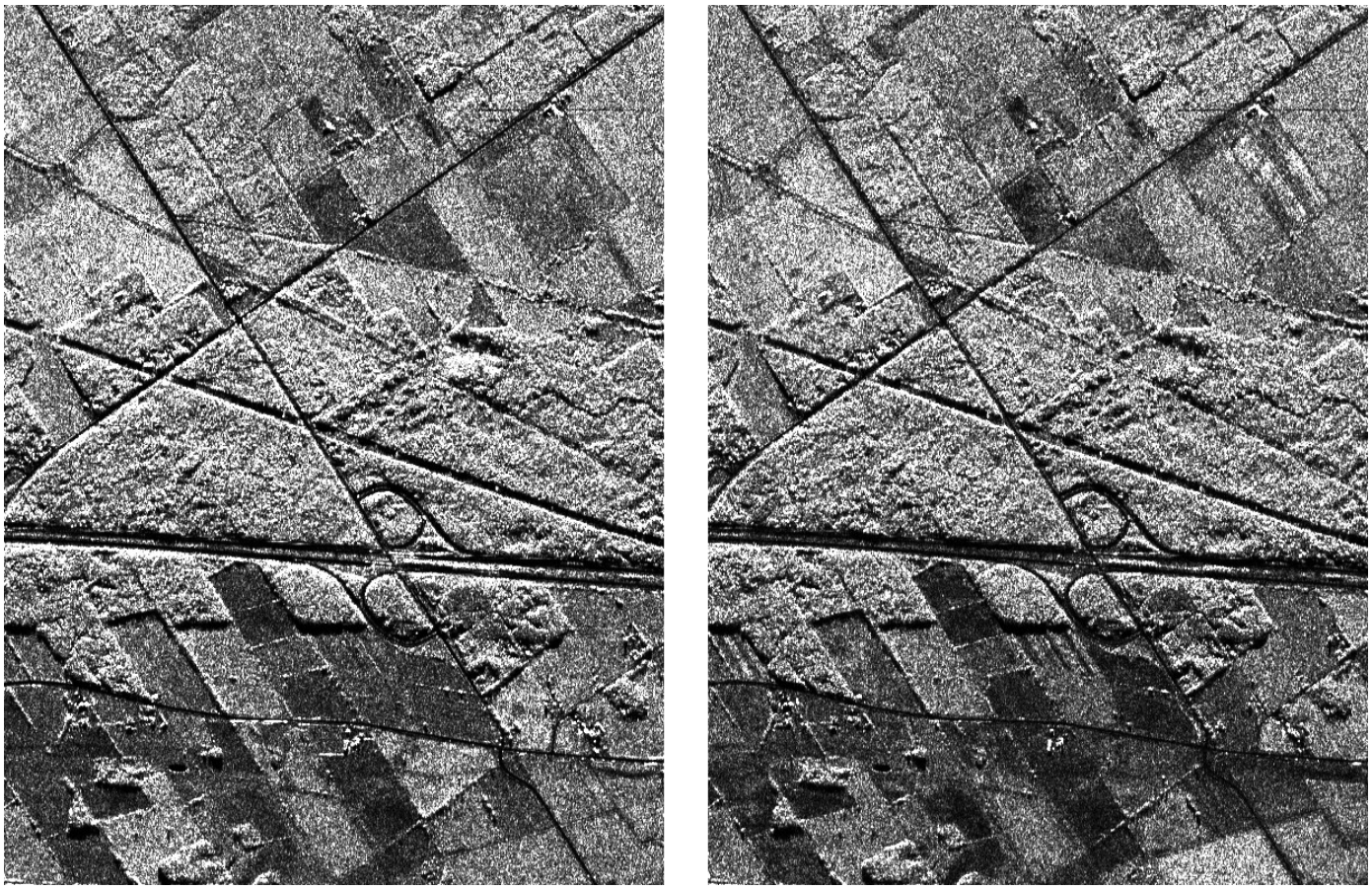

Fig. 3. The image of the Mer Bleu area (600x800 pixels). The amplitudes of the hh channel (left) and the vv channel (right) of 9-look polarimetric SAR data are shown. The image is obtained from polarimetric Convair-580 SAR data collected over the Ottawa region, Canada.

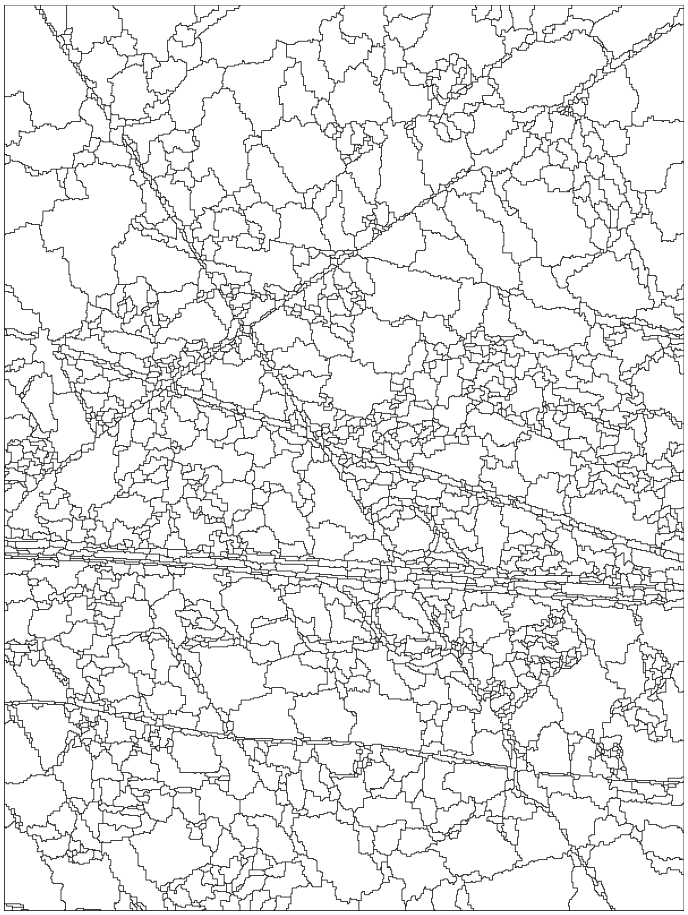

Fig. 4. Partition with 2000 segments produced by the Wishart stepwise criterion.

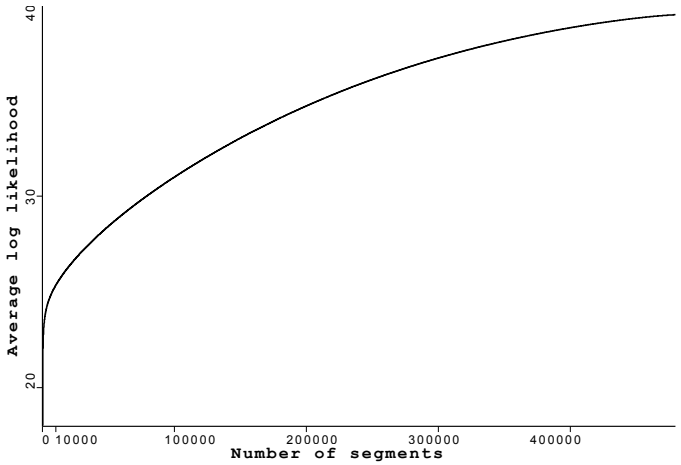

Fig. 5. Average log likelihood of a partition as a function of the number of segments for the Wishart model.

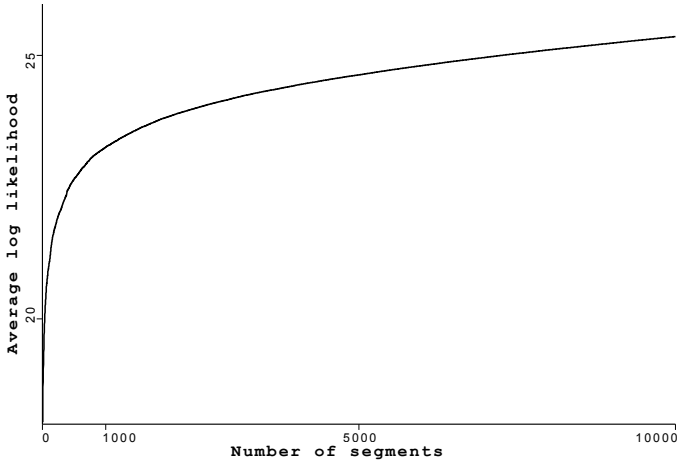

Fig. 6. Average log likelihood values for partitions that have a number of segments between 1 and 10,000.

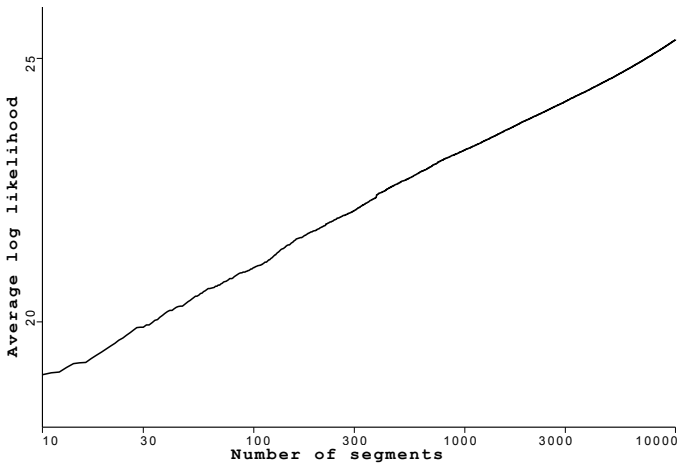

Fig. 7. Average log likelihood values as a function of the log of the partition size.

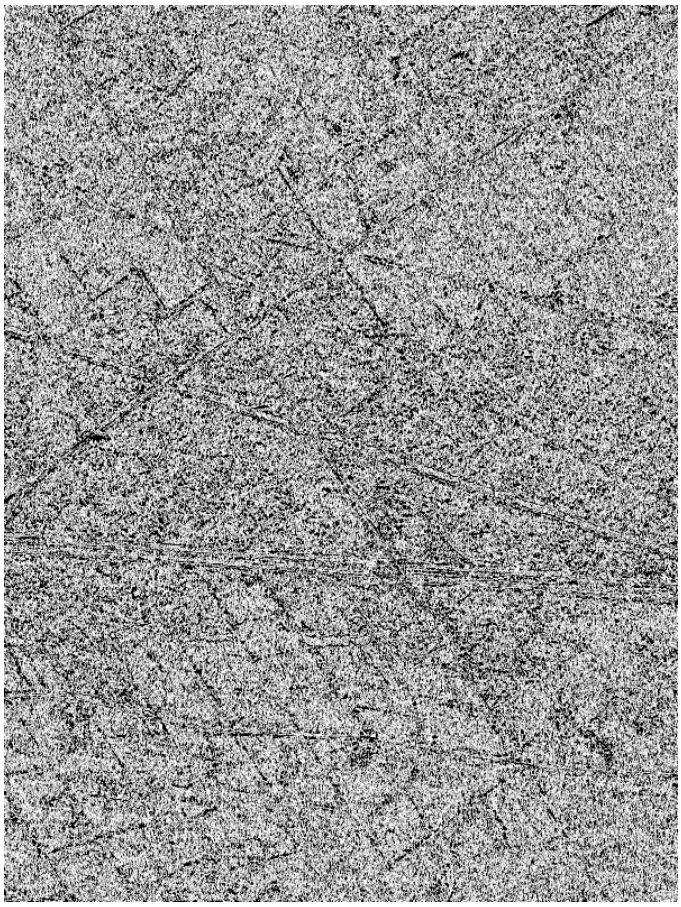

Fig. 8. Normalized log likelihood image for the partition of Fig. 4.

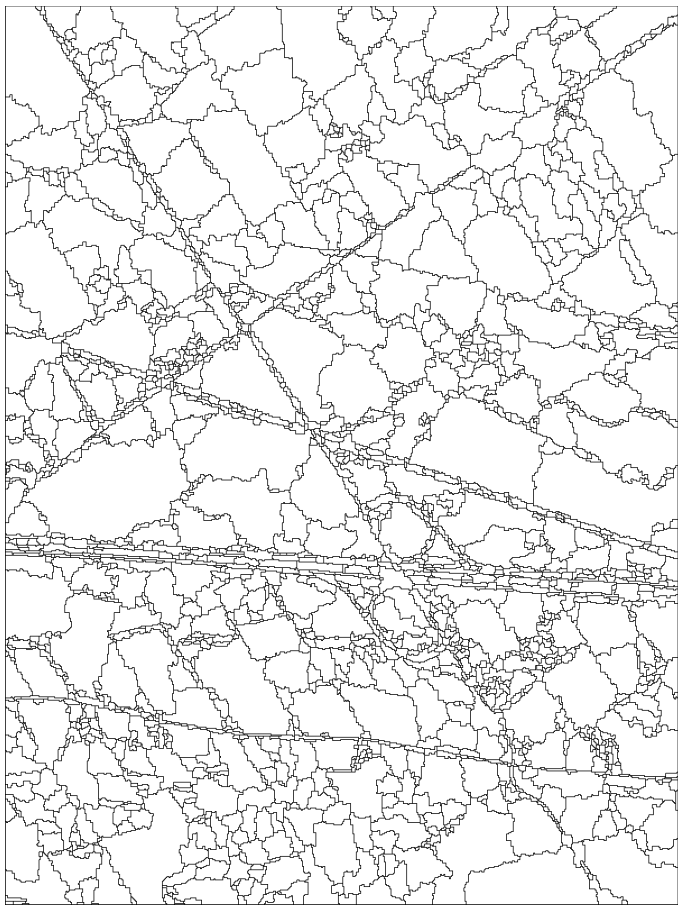

Fig. 9. Partition with 2000 segments produced by the combination of the Wishart and K distribution stepwise criteria.

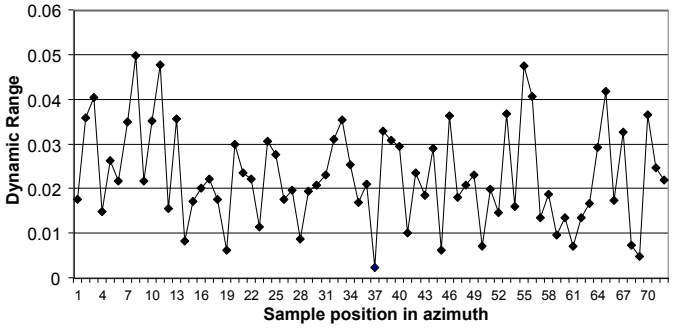

Fig. 10. Between channel dynamic range of variation coefficient for a forest area.